Thermochemistry of Oxo Transfer from Coordinated Nitrite in the Dinitro(5,10,15,20-tetrakis(*o*-pivalamidophenyl)porphinato)iron(III) Anion

Melanie Frangione, Jennifer Port, Murtuza Baldiwala, Andrew Judd, John Galley, Magrey DeVega, Kara Linna, Leigh Caron, Elizabeth Anderson, and John A. Goodwin*

Collegium of Natural Sciences, Eckerd College, St. Petersburg, Florida 33733

Received July 25, 1996[⊗]

The thermochemistry of oxo transfer from coordinated nitrite in the dinitro(5,10,15,20-tetrakis(*o*-pivalamidophenyl)-porphinato)iron(III) anion, ion-paired with the tetrapropylammonium ion, $\{[Fe^{III}TpivPP(NO_2)_2]^-Pr_4N^+\}$, has been evaluated in acetonitrile solution. This oxo-transfer half-reaction of $\{[Fe^{III}TpivPP(NO_2)_2]^-Pr_4N^+\}$ has been assessed on the basis of the determination of the $E_{1/2} = +0.54$ V vs SHE for the reversible $[Fe^{II/III}TpivPP(NO)(NO_2)]^{-/0}$ couple and the measurement of the formation constants for the association of NO and NO_2^- with the mononitroiron(III) porphyrin derivative. The formation constant for nitric oxide association, K_{NO}, has the value $(1.21 \pm 0.08) \times 10^3$. The stability constant, K_2, for association of a second nitro ligand in 0.0100 M tetrapropylammonium perchlorate medium has been estimated as 2.18×10^3. The oxo-transfer half-reaction free energy, $\Delta G°_{(X/XO)}$, for *addition* of oxygen to $[Fe^{II}TpivPP(NO)(NO_2)]^-$ to form $\{[Fe^{III}TpivPP(NO_2)_2]^-Pr_4N^+\}$ has been found to be −50 kJ/mol.

Introduction

Secondary oxygen atom transfer, oxo transfer, has been observed in many transition metal-coordinated nitrite systems[1] including the ion-paired chloronitro(tetraphenylporphinato)-iron(III) anion, which is capable of oxidizing dioxygen to *ozone*.[2] Not all ferric nitro porphyrins display this reactivity, however. The dinitroiron(III) picket fence porphyrin anion,[3] $[Fe^{III}TpivPP(NO_2)_2]^-$ (**1**), is stable with dioxygen in acetonitrile solution but reacts with strong oxo-acceptors such as triphenylphosphine,[4,5] nitric oxide,[6] and thiophenols.[7] These reducing agents all produce nitrosyliron(II) picket fence porphyrin by way of biphasic reactions[5] in which the observable intermediate is proposed to be the nitronitrosyliron(II) picket fence porphyrin anion, $[Fe^{II}TpivPP(NO)(NO_2)]^-$, (**2**).

To understand the different reactivities of nitro porphyrin complexes toward dioxygen and other oxygen-accepting substrates, X, requires measurement of the driving forces for oxo transfer. A model oxo-transfer reaction we have evaluated with the picket fence derivative is given in eq 1. This system uses triphenylphosphine as a strong oxo acceptor, X, since the thermodynamics of eq 2 have been studied and since the product of eq 1 is relatively long-lived in the reaction with triphenylphosphine.[5] This intermediate, which is assigned as **2**, $[Fe^{II}TpivPP(NO)(NO_2)]^-$, and its oxidized analogue, $[Fe^{III}TpivPP(NO)(NO_2)]$, have been characterized in solution in this work by cyclic voltammetry.

$$\underset{\mathbf{1}}{[Fe^{III}TpivPP(NO_2)_2]^-} + Ph_3P \rightarrow \underset{\mathbf{2}}{[Fe^{II}TpivPP(NO)(NO_2)]^-} + Ph_3PO \quad (1)$$

$$Ph_3P + {}^1/_2O_2 \rightarrow Ph_3PO \quad (2)$$

$$[Fe^{III}TpivPP(NO_2)_2]^- \rightarrow [Fe^{II}TpivPP(NO)(NO_2)]^- + {}^1/_2O_2 \quad (3)$$

Equation 3 corresponds to the reduction of the $[Fe^{III}TpivPP(NO_2)_2]^-$ anion to **2** by its loss of an oxygen atom.[8] The driving force for eq 3 has been determined indirectly by combining results of equilibrium and electrochemical measurements and appears to be the first measurement of this kind for a coordinated nitro ligand.[9] Combining the free energies of eqs 2 and 3 yields the free energy for the overall oxo-transfer reaction in eq 1. Similar combinations of the free energy of eq 3 with known $\Delta G°_{(X/XO)}$ values permits explanation of the characteristic stability of the dinitroiron(III) picket fence porphyrin anion toward decomposition by free nitrite and dioxygen.

Experimental Section

General Methods. All preparations and measurements were carried out under nitrogen or mixed nitrogen−nitric oxide atmosphere by using either a nitrogen-filled glovebox that was configured with a fiber-optic spectrometer (Ocean Optics, PC1000) or a Schlenk line and syringe

* Author to whom correspondence should be addressed. Present address: Department of Chemistry, Coastal Carolina University, P.O. Box 261954, Conway, SC 29528-6045.

[⊗] Abstract published in *Advance ACS Abstracts,* April 1, 1997.

(1) Tovrog, B. S.; Diamond, S. E.; Mares, F. *J. Am. Chem. Soc.* **1979**, *101*, 270−272. Diamond, S. E.; Mares, F.; Szalkiewicz, A.; Muccigrosso, D. A.; Solar, J. P. *J. Am. Chem. Soc.* **1982**, *104*, 4266−4268. Pipes, D. W.; Meyer, T. J. *Inorg. Chem.* **1984**, *23*, 2466−2472. Younathan, J. N.; Wood, S. K.; Meyer, T. J. *Inorg. Chem.* **1992**, *31*, 3280−3285. Toth, J. E.; Anson. F. C. *J. Am. Chem. Soc.* **1989**, *111*, 2444−2451. Rhodes, M. R.; Barley, M. H.; Meyer, T. J. *Inorg. Chem.* **1991**, *30*, 629−635. Keene, F. R.; Salmon, D. J.; Walsh, J. L.; Abruna, H. D.; Meyer, T. J. *Inorg. Chem.* **1980**, *19*, 1896−1903.

(2) Castro, C. E. *J. Am. Chem. Soc.* **1996**, *118*, 3984−3985.

(3) Nasri, H.; Goodwin, J. A.; Scheidt, W. R. *Inorg. Chem.* **1990**, *29*, 185−191.

(4) Mashuta, M.; Scheidt, W. R. University of Notre Dame, personal communication, 1992.

(5) Goodwin, J. A. Manuscript in preparation. All of these reactions in acetonitrile solvent ultimately produce the ferrous nitrosyl derivative, $[Fe^{II}TpivPP(NO]$; however, stopped-flow kinetics of the reaction of **1** with nitric oxide and thiophenols show a much faster decay of the intermediate than in the reaction with triphenylphosphine.

(6) Goodwin, J. A.; Stanbury, D. M. Unpublished results, July 1991.

(7) Nasri, H.; Haller, K.; Wang, W.; Huynh, B. H.; Scheidt, W. R. *Inorg. Chem.* **1992**, *31*, 3459−3467.

(8) The reverse of eq 3 is used later in this paper in following the convention for the half-reaction free energy, $\Delta G°_{(X/XO)}$, in which the acceptor X reacts with ${}^1/_2O_2$ to form XO.

(9) Review of the literature to July 1996 revealed no previous measurements of this type.

S0020-1669(96)00891-9 CCC: $14.00

techniques. All equilibria were studied by absorbance methods in acetonitrile solution as detailed below. Solutions of nitric oxide were made by sparging with solvent-saturated mixtures of NO and N_2 prepared with a stainless steel proportioner (Matheson). Concentrations of nitric oxide were determined by partial pressures of NO in N_2, according to Henry's law given for NO in acetonitrile by Shaw and Vosper.[10]

Acetonitrile (AN) was sequentially distilled from anhydrous $CuSO_4$ and CaH_2 and then stored under nitrogen and dried with activated alumina immediately before use. Tetrapropylammonium nitrite ((TPA)NO_2) and tetrapropylammonium perchlorate ((TPA)ClO_4) were prepared according to literature methods,[11] analyzed for traces of bromide starting material by cyclic voltammetry, and dried before use. Tetrapropylammonium perchlorate was purified according to literature methods.[12] The UV−visible spectrum of tetrapropylammonium nitrite was consistent with that reported by Strickler and Kasha.[13] This absorbance band (λ_{max} = 369 nm, ϵ_{369} = 24.2 M^{-1} cm^{-1}) was routinely used for determination of the nitrite solution concentration in acetonitrile.

Syntheses. Triflatoiron(III) picket fence porphyrin monohydrate, [Fe^{III}TpivPP(O_2SOCF_3)]·H_2O, was prepared according to the literature method[14] from the bromoiron(III) picket fence porphyrin obtained from Midcentury Chemicals and used as received. The dinitroiron(III) picket fence porphyrin anion, [Fe^{III}TpivPP(NO_2)$_2$]$^-$ (**1**), was prepared in solution by addition of (TPA)NO_2 to solutions of [Fe^{III}TpivPP(O_2SOCF_3)]·H_2O with (TPA)ClO_4 electrolyte. Both **1** and the equilibrium species mononitroiron(III) picket fence porphyrin, [Fe^{III}TpivPP(NO_2)] (**3**), have been characterized in detailed equilibrium studies described below and previously.[3]

The unstable nitronitrosyliron(II) picket fence porphyrin anion, [Fe^{II}TpivPP(NO)(NO_2)]$^-$ (**2**), was prepared in acetonitrile solution by reaction of **1** with excess triphenylphosphine and was characterized by its UV−visible absorbance spectrum in CH_3CN. Its rapid formation was observed by stopped-flow UV−visible spectrophotometry at 420 nm using a CAN-Tech TDI Model 2A stopped-flow apparatus and data acquisition system. Solutions of the weakly coordinated triflatoiron(III) porphyrin were also combined with Ph_3P in acetonitrile to compare the product spectra. No changes in the UV−visible spectrum of [Fe^{III}TpivPP(OSO_2CF_3)] were evident upon that addition.

Nitrosyliron(II) picket fence porphyrin, [Fe^{II}TpivPP(NO)] (**4**), was prepared by adaptation of a procedure used for the preparation of the tetraphenylporphyrin (TPP) derivative in pyridine solvent using Schlenk techniques.[15] The starting material, bromoiron(III) picket fence porphyrin (Midcentury) was used as received. Due to solubility differences with the TPP derivative, the ratios of solvents used in the reductive nitrosylation and recrystallization steps were modified from the original procedure. For recrystallization, chloroform solutions were maintained under a nitric oxide atmosphere while methanol and hexane were added for overall proportions of 2:1:4. The resulting solution was reduced in volume until purple crystals formed. The solid was collected and chromatographed with basic alumina using toluene (EM, distilled) and then recrystallized from toluene solution with hexane. Spectroscopic characterizations by IR (KBr pellet) and UV−visible (chloroform) were consistent with previous reports of the picket fence porphyrin derivative obtained by an indirect method.[7]

Determination of Stability Constants. (i) Nitrite Association. The determination of nitrite association constants with iron picket fence porphyrin was carried out under nitrogen using a fiber-optic UV−visible spectrometer configured for use in a nitrogen-filled glovebox. Due to the sensitivity to water contamination of the weakly coordinated triflatoporphyrin [Fe^{III}TpivPP(O_2SOCF_3)] in acetonitrile, all titrations for the determination of nitrite association constants were begun with roughly equal proportions of porphyrin and nitrite in solutions having (TPA)ClO_4 as the ionic strength medium held at 0.010 06 M. These solutions were titrated with second solutions having roughly equal concentrations of porphyrin but a large excess of nitrite and constant (TPA)ClO_4 concentration. Additions of solutions containing excess nitrite were made with a microliter pipet or a Hamilton syringe. Porphyrin concentrations were determined by use of literature values[3] for the dinitroiron(III) porphyrin complex in dichloromethane by preparing solutions with a large excess of nitrite at high ionic strength. Concentrations of the porphyrin ranged around 6×10^{-5} M throughout the titrations due to slight differences in porphyrin concentration in the two solutions, but the concentration of nitrite ranged from 5×10^{-5} to 5×10^{-3} M. The analytical concentrations of porphyrin, nitrite, and electrolyte in each addition were treated explicity in data analysis. Contributions of ion pairing of (TPA)NO_2 and (TPA)ClO_4 were considered in all equilibrium measurements and calculations.[16] No corrections were necessary for ionic association of the nitrite ion with the tetrapropylammonium cation. However, due to ion pairing, the calculated concentration of the free perchlorate ion in the titration was 0.009 171 M. Analysis of the absorbance changes at six wavelengths was carried out for eight of the UV−visible spectra collected during the titration using the PC version of the FORTRAN program SPECDEC.[17]

(ii) Nitric Oxide Association. Determination of the equilibrium constant for coordination of NO to **3** was achieved by anaerobic UV−visible methods using a 2 mm quartz cuvette that was attached to a high-vacuum Teflon stopcock with a 9 mm O-ring joint. A side port above the stopcock seal allowed additions through a septum under the flow of the gas mixture. No ionic strength medium was added to these solutions to simplify the equilibrium conditions. Saturated acetonitrile solutions of NO/N_2 were added by gas-tight syringe to solutions of **3** in the anaerobic cuvette and the absorbance values at 434 nm recorded immediately. Corrections to the absorbance values were made for dilution. The nonlinear dependence of the absorbance at 434 nm upon NO concentration was carried out as detailed below using the SigmaPlot 4.1 for DOS as descibed in the Results and Discussion section.

Determination of Half-Wave Potentials. All electrochemical experiments were carried out by cyclic voltammetry with acetonitrile solutions containing 0.0500 M (TPA)ClO_4 using an EG&G VersaStat potentiostat and a sweep rate of 20 mV/s. A platinum working electrode and a Ag/$AgNO_{3(AN)}$ reference electrode (Cypress Systems) were used for all measurements to avoid contamination with water. Reference electrode conversions from Ag/$AgNO_{3(AN)}$ to SHE were made by internal reference measurements of $E_{1/2}$ = 0.071 V for ferrocene. The same reference solution was tested with an aqueous Ag/AgCl electrode with $E_{1/2}$ = 0.51 V. The latter reference electrode was taken to have a potential of +0.197 V vs SHE. Solutions of porphyrins (1×10^{-4} M) prepared for electrochemical experiments were sparged for at least 30 min with solvent-saturated nitrogen or NO/N_2 gas mixtures. Equilibrium solutions of [Fe^{III}TpivPP(NO_2)(ClO_4)] (**3a**), described below, were prepared by adding 1.2×10^{-4} M (TPA)NO_2 to the porphyrin/electrolyte solutions. For generation of stable solutions of **5**, 15 mM nitric oxide gas was sparged through solutions of **3a**.

Results and Discussion

General Characterization of Porphyrins in Solution by UV−Visible Spectroscopy. The dinitroiron(III) picket fence porphyrin anion, [Fe^{III}TpivPP(NO_2)$_2$]$^-$ (**1**), has been previously characterized in the solid state by X-ray diffraction and in solution in chlorinated solvents by a range of spectral techniques.[3] Figure 1A shows the visible spectrum of the complex

(10) Shaw, A. W.; Vosper, A. J. *J. Chem. Soc. (A)* **1971**, 1592−1595.
(11) Kobler, H.; Munz, G.; Simchen. G. *Liebigs Ann. Chem.* **1978**, 1937.
(12) Perrin, D. D.; Armanego, W. L. F. *Purification of Laboratory Chemicals*, 3rd ed.; Pergamon: Oxford, 1988.
(13) Strickler, S. J.; Kasha, M. *J. Am. Chem. Soc.* **1963**, *85*, 2899−2901.
(14) Gismelseed, A.; Bominaar, E. L.; Bill, E.; Trautwein, A. X.; Winkler, H.; Nasri, H.; Doppelt, P.; Mandon, D.; Fischer, J.; Weiss, R. *Inorg. Chem.* **1990**, *29*, 2741−2749.
(15) Scheidt, W. R.; Frisse, M. E. *J. Am. Chem. Soc.* **1975**, *97*, 17−21.
(16) A nonlinear least-squares fit of the apparent conductivity versus analytical concentration of (TPA)NO_2 gave the value of the dissociation constant for the ion pair, K_{diss}, (1.71 ± 0.03) × 10^{-2}, with a limiting conductivity of (1.70 ± 0.02) × 10^2 S cm^2 mol^{-1}. The dissociation constant is comparable to earlier reports of K_{diss} for (TPA)I_3 of 1.08×10^{-2}. Considering the experimental concentrations used and ionic strength effects, contributions of ion pairing to the analytical concentrations of nitrite were negligible. Ion pairing of the supporting electrolyte was not measured, but the value of the dissociation constant, K_{diss} = 0.10, reported for Bu_4NBF_4 in acetonitrile[19] was used as an approximation.
(17) Atkins, C. E.; Park, S. E.; Blaszek, J. A.; McMillin, D. R. *Inorg. Chem.* **1984**, *23*, 569−572.

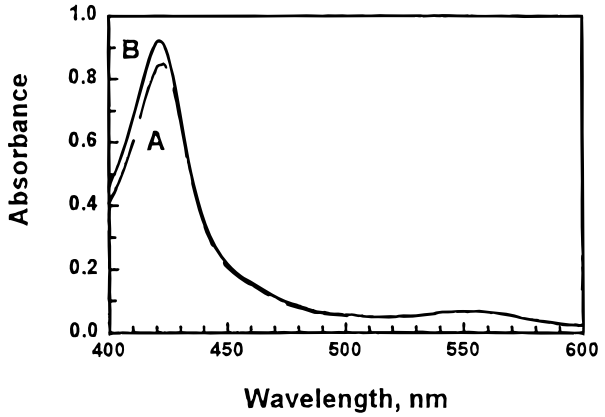

Figure 1. (A) Visible spectrum of the dinitroiron(III) picket fence porphyrin anion, $[Fe^{III}TpivPP(NO_2)_2]^-$ (**1**), in acetonitrile solution at 3.9×10^{-5} M, $[(TPA)NO_2] = 3.3$ mM, $[(TPA)ClO_4] = 0.50$ M; path length = 1 mm. (B) Visible spectrum assigned as $[Fe^{II}TpivPP(NO)(NO_2)]^-$ (**2**), obtained as the product of the spectrum A immediately after addition of triphenylphosphine (25 mM), $t = 30$ s, corrected for dilution.

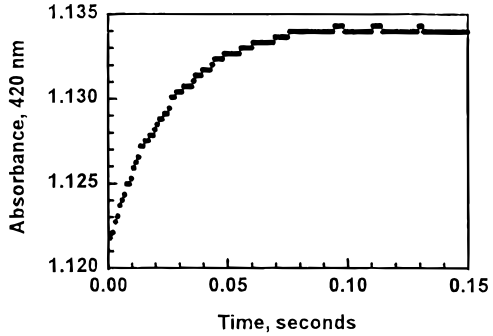

Figure 2. Rapid absorbance change accompanying the reaction of the dinitroiron(III) picket fence porphyrin anion, $[Fe^{III}TpivPP(NO_2)_2]^-$ (**1**), with triphenylphosphine in acetonitrile/$(TPA)ClO_4$ medium, obtained by stopped-flow spectrophotometry under nitrogen. Observation wavelength = 420 nm, porphyrin concentration $= 7.5 \times 10^{-5}$ M, $[(TPA)NO_2] = 5 \times 10^{-3}$ M, $[Ph_3P] = 2.5 \times 10^{-2}$ M; observation path length = 6.2 mm.

in acetonitile−electrolyte solution which is nearly identical to the previous results. However, the formation of the $[Fe^{III}TpivPP(NO_2)_2]^-$ anion (**1**) shows a particular dependence on the presence of electrolyte in acetonitrile medium that was not apparent in the chlorinated solvents of the previous work.[3] This dependence is discussed in the equilibrium studies later in this section. The equilibrium involves mononitroiron(III) picket fence porphryin, $[Fe^{III}TpivPP(NO_2)]$ (**3**), which has also been observed previously but not isolated.[3] A spectrum of a solution of this equilibrium species is shown in Figure 4A.

Formation of $[Fe^{II}TpivPP(NO)(NO_2)]^-$ (**2**) as an intermediate in the reaction of triphenylphosphine with **1** has been followed by UV−visible spectroscopy. The visible spectrum that results immediately upon the addition of triphenylphosphine to acetonitrile solutions of **1** is shown in Figure 1B. Rapid formation of the product is evident, with a Soret peak at 421 nm and a peak at 555 nm that is distinguishable from the spectrum of the reactant $[Fe^{III}TpivPP(NO_2)_2]^-$, primarily by the increase in molar absorptivity and the slight shift from a maximum at 424 nm to the lower wavelength. The increase in absorbance at 420 nm over the period of 0−0.15 s obtained by stopped-flow spectrophotometry is shown in Figure 2. These first-order kinetics data were obtained under conditions of excess triphenylphosphine at a concentration of 0.025 M and yield an estimate of the bimolecular rate constant of 1×10^3 M^{-1} s^{-1}.[5] The subsequent slow decay of the intermediate assigned as **2** to $[Fe^{II}TpivPP(NO)]$ (**4**) is shown in Figure 3. The product **4** is assigned on the basis of the characteristic Soret band position at 406 nm. The series of spectra in Figure 3 were obtained over 7 h hours under anaerobic conditions.[18]

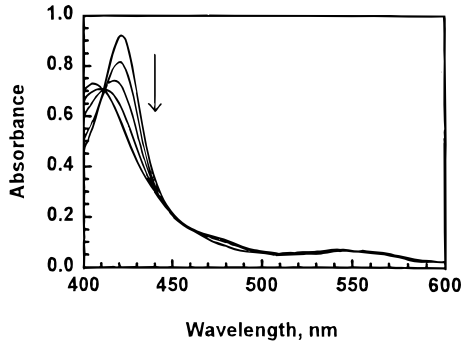

Figure 3. Visible spectra accompanying the decomposition of $[Fe^{II}TpivPP(NO)(NO_2)]^-$ (**2**), shown in Figure 1B, to $[Fe^{II}TpivPP(NO)]$ (**8**) under anaerobic conditions. Spectra acquired in the order indicated by the arrow were collected at times of 30 sec, 24 min, 57 min, 90 min, and 7 h.

The oxidized derivative of **2**, the nitronitrosyliron(III) picket fence porphyrin anion, $[Fe^{III}TpivPP(NO)(NO_2)]$ (**5**), has also been characterized in this work by visible spectroscopy, equilibrium binding studies, and cyclic voltammetry. Figure 4B shows the visible spectrum of **5** that results upon the reversible addition of nitric oxide to $[Fe^{III}TpivPP(NO_2)]$ in acetonitrile solution. Details of the coordination equilibrium of NO and the electrochemistry of **5** are given later in this section.

Equilibrium Studies. In the treatment of the absorbance data obtained for nitrite coordination experiments with the SPECDEC program, two-parameter fits for the sequential coordination of nitrite to the free porphyrin, as shown in eqs 4a and 5a, were initially attempted with no explicit dependence on concentration of the supporting electrolyte. The terms Q_{1a}

$$\underset{\mathbf{6}}{[Fe^{III}TpivPP]^+} + NO_2^- \rightarrow \underset{\mathbf{3}}{[Fe^{III}TpivPP(NO_2)]} \qquad Q_{1a} \quad (4a)$$

$$[Fe^{III}TpivPP(NO_2)] + NO_2^- \rightarrow \underset{\mathbf{1}}{[Fe^{III}TpivPP(NO_2)_2]^-} \qquad Q_{2a} \quad (5a)$$

and Q_{2a} are the conditional equilibrium quotients for these two reactions. Species **6** was assumed to be uncoordinated in this model regardless of any weak association of the triflate ion, the perchlorate ion, or the acetonitrile solvent. In these fits, the molar absorptivities of the uncomplexed porphyrin, **6**, in solution were held fixed as determined by the absorbance spectrum of the triflate derivative in chloroform. The relatively poor fit obtained by this model is reflected in the large value of 7×10^{-2} for χ^2 provided by the SPECDEC program. The results of this simple model were not used.

In preparation of solutions of $[Fe^{III}TpivPP(NO_2)_2]^-$ in CH_3CN, it was obvious that higher concentrations of supporting electrolyte allowed the expected UV−visible spectrum with the

(18) The small deviation from isosbestic behavior apparent in Figure 2 has been evaluated by treating the biphasic absorbance at 10 wavelengths, ranging from 390 to 435 nm. For the reaction, formation of $[Fe^{II}TpivPP(NO)]$ occurs with an observed first-order rate constant of 5×10^{-5} s^{-1}. A second reaction, which produces an unidentified nitro complex or mixture of complexes, occurs with an observed rate constant of 1×10^{-5} s^{-1}. The final spectrum depends on nitrite concentration, but the identity of product(s) and details of this decomposition reaction are as yet unknown.

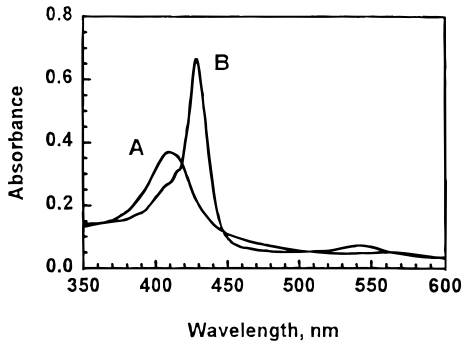

Figure 4. (A) Visible spectrum of mononitroiron(III) picket fence porphyrin, [Fe^{III}TpivPP(NO$_2$)] (1.5×10^{-5} M), in acetonitrile, path length = 1 cm, sealed under nitrogen. (B) Change in visible spectrum A upon reaction with NO (7.5 mM), obtained by immediate collection of the spectrum after injection of an equal volume of saturated NO solution in acetonitrile and correcting for dilution.

characteristic Soret position at 424 nm to be observed at lower concentrations of nitrite. Additionally, variability in the spectrum of the acetonitrile solutions of the triflate complex suggested coordination by solvent, contaminant water, and perchlorate. Titrations of (TPA)ClO$_4$ did, indeed, show shifts in the variable Soret position from 412−416 to 408−410 nm, but variability suggested continued competing equilibria. These observations and the poor fits obtained in the simple model of eqs 4a and 5a suggested that association of the electrolyte should be considered explicitly in this coordination equilibrium. Furthermore, previous evidence of specific ion pairing in other solvents[3] prompted more complicated evaluation. An equilibrium model based on eqs 4b, 5b, and an additional reaction, given in eq 6, was developed for evaluation with the SPECDEC program. In this model, the perchlorate ligand's concentration

$$[\mathrm{Fe^{III}TpivPP}]^+ + \mathrm{ClO_4}^- \rightarrow [\mathrm{Fe^{III}TpivPP(ClO_4)}] \qquad Q_{0b} \quad (6)$$
6 **7**

$$[\mathrm{Fe^{III}TpivPP(ClO_4)}] + \mathrm{NO_2}^- \rightarrow [\mathrm{Fe^{III}TpivPP(ClO_4)(NO_2)}]^- \qquad Q_{1b} \quad (4b)$$
7 **3a**

$$[\mathrm{Fe^{III}TpivPP(ClO_4)(NO_2)}]^- + \mathrm{NO_2}^- + \mathrm{Pr_4N}^+ \rightarrow \{[\mathrm{Fe^{III}TpivPP(NO_2)_2}]^-\mathrm{Pr_4N}^+\} + \mathrm{ClO_4}^- \qquad Q_{2b} \quad (5b)$$
3a **1a**

dependence in formation of a spectroscopically distinct perchloratoiron(III) porphyrin (**7**) was assessed. Reactions 4 and 5 were modified to include the new species **7**. The ion-paired species **1a**, which consists of the dinitroiron(III) picket fence porphryin anion and the tetrapropylammonium ion was introduced in eq 5b. The term Q_{0b} is the conditional stability quotient for the formation of the perchlorato complex, and Q_{2b} now includes both nitrite association and the ion-pairing equilibrium. Much improved fits, with $\chi^2 = 1.19 \times 10^{-3}$, were obtained with these changes. Models with separate terms for the reactions in eq 5b showed no improvement in the fit and were not able to resolve distinct equilibrium quotients for dissociation of perchlorate from **3a** prior to association of the second nitrite ligand.

Values for all the fitted association quotients, Q_{nb}, determined in this latter model (eqs 4b, 5b, and 6) are listed in Table 1. The calculated molar absorptivities for each of the equilibrium porphyrin species, **6**, **7**, **3a**, and **1a**, are shown with interpolated

Table 1. Values of Stability Constants for Perchlorate and Nitrite Association to Iron(III) Picket Fence Porphyrin in Acetonitrile

	$n = 0$	$n = 1$	$n = 2$
Q_{nb}[a]	1.86×10^3	4.25×10^6	2.87×10^3
K_{nb}[b]	3.24×10^3	5.35×10^6	2.18×10^3
K_n[c]		1.49×10^4	4.0×10^4

[a] Results of this work according to eqs 6, 4b, and 5b, CH_3CN solution, 0.010 06 M (TPA)ClO$_4$, uncorrected for ionic strength. The designation $n = 0$ refers to no nitro ligands but one perchlorato ligand; $n = 2$ and 3 refer to the stepwise coordination equilibria of nitrite. [b] Stability constants corrected to zero ionic strength by activity coefficients calculated by eq 7. [c] Previous measurement (ref 3), CH_2Cl_2 solution with no ionic strength medium. Ion size parameters, *a*, and activity coefficients, *f*, for 0.010 06 M (TPA)ClO$_4$ that were used in determining corrections of the conditional equilibrium quotients to zero ionic strength are given for the following ions: ClO_4^-, Pr_4N^+, NO_2^-, and all singly charged porphyrins P^-. The *a* values are 3.5, 8, 3, and 12, respectively. The *f* values are 0.7304, 0.7650, 0.7259, and 0.7891, respectively.

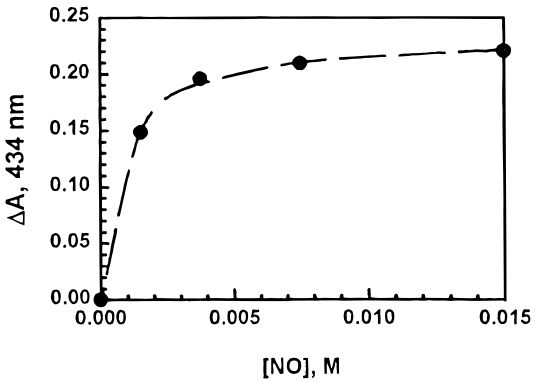

Figure 5. Changes in absorbance at 434 nm upon addition of nitric oxide to [Fe^{III}TpivPP(NO$_2$)] in acetonitrile. The conditions are the same as those described in Figure 4. Observed changes in absorbance shown with the ● symbols are defined as the difference between the measured absorbance and absorbance of the initial mononitroiron(III) picket fence porphyrin solution, corrected for dilution. The dashed line corresponds to the the best fit of the data to eq 9. This calculation gave $K_{NO} = (1.21 \pm 0.08) \times 10^3$ and $\Delta\epsilon = (1.56 \pm 0.02) \times 10^5$ M^{-1} cm^{-1}.

spectra in Figure 6A−D. Corrections to these equilibrium quotients for ionic strength using Debye−Hückel theory were applied to estimate the thermodynamic values of the equilibrium constants, K_{na}, at zero ionic strength. Activity coefficients, γ, for the ionic species were determined by eq 7 using ion size parameters, *a*, listed in Table 1. These values of *a* are estimates

$$\log(\gamma) = -Az^2\mu^{1/2}/(1 + Ba\mu^{1/2}) \qquad (7)$$

only, as they were taken from values for aqueous media. The porphyrin *a* value is also an estimate. The values[19] $A = 1.646$ M$^{-1/2}$, $B = 0.486$ M$^{-1/2}$ Å^{-1} were used in these calculations. The resulting activity coefficients, γ, are listed in Table 1B. Expressions for the thermodynamic stability constants for association of nitrite alone, as implied by the simpler expressions of eqs 4a and 5a, are more useful for comparision with literature values and for the thermochemical cycle presented later. These terms will be approximated as $K_1 = K_{1b} = 5.35 \times 10^6$ and $K_2 = K_{2b} = 2.18 \times 10^3$. Comparisons of these values of K_0,[20] K_1, and K_2 to literature values[3] are also listed in Table 1. Reference numbers **1** and **1a** will be used interchangeably to designate the ion-paired equilibrium of **1** and **1a** in the remainder of this paper.

(19) Goodwin, J. A.; Stanbury, D. M.; Wilson, L. J.; Eigenbrot, C. W.; Scheidt, W. R. *J. Am. Chem. Soc.* **1987**, *109*, 2979−2991.

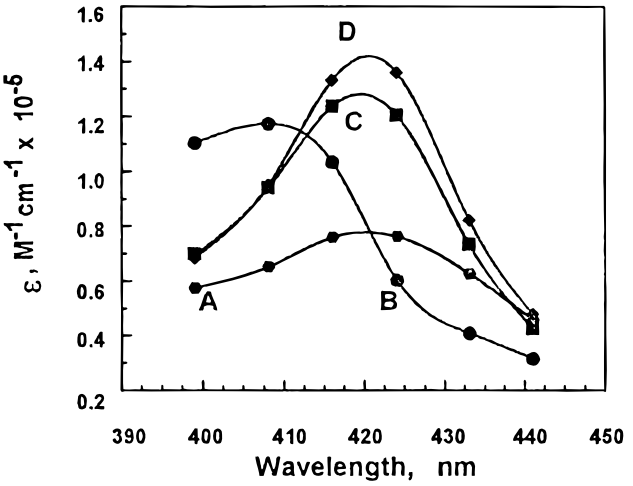

Figure 6. Calculated molar absorptivities, ϵ (M^{-1} cm^{-1}, symbols), and interpolated spectra (natural spline fit) obtained from the SPECDEC analysis of the titration of [Fe^{III}TpivPP(O_2SOCF_3)] (6×10^{-5} M) with tetrapropylammonium nitrite (5×10^{-5}−5×10^{-3} M) in 0.010 06 M tetrapropylammonium perchlorate−acetonitrile medium under nitrogen atmosphere at 25 °C, as described by eqs 4b, 5b, and 6. Calculated molar absorptivies shown by the labeled lines correspond to the equilibrium species as follows: (A) the uncomplexed [Fe^{III}TpivPP]$^+$ (**6**), held fixed in the SPECDEC calculation; (B) [Fe^{III}TpivPP(ClO_4)] (**7**); (C) [Fe^{III}TpivPP(NO_2)(ClO_4)]$^-$ (**3a**); and (D) {[Fe^{III}TpivPP-(NO_2)$_2$]$^-$$Pr_4N^+$} (**1a**).

Association Equilibrium of [Fe^{III}TpivPP(NO_2)] with Nitric Oxide. Figure 4 illustrates the change in the position of the Soret band that accompanies the reaction of NO with **3** according to eq 8. Note that supporting electrolyte was not

$$\underset{\mathbf{3}}{[Fe^{III}TpivPP(NO_2)]} + NO_{(g)} \rightarrow \underset{\mathbf{5}}{[Fe^{III}TpivPP(NO_2)(NO)]} \quad (8)$$

added to this system as a simplification of the equilibrium, so that species **3** and not **3a** is specified in eq 8. The resulting peak position at 434 nm is comparable to that observed by Settin and Fanning[21] for the FeTPP derivative and by Yoshimura[22] for the FeTPP and the iron protoporphyrin(IX) methyl ester derivative. This addition of NO occurs on the stopped-flow time scale[6] and results in a change in absorbance that appears to be completely reversible, with regeneration of the spectrum of the starting material upon sparging with nitrogen. If NO is constantly bubbled through the solution, the ferric species is stable for hours. The changes in absorbance at 434 nm that occur upon incremental additions of nitric oxide are shown in Figure 5. Equation 9 shows the relationship between the change in absorbance, ΔA, and the two parameters K_{NO}, the equilibrium constant, and $\Delta\epsilon$, the change in molar absorptivity, where $b = K_{NO}([Fe]_0 + [NO]_0) + 1$. The term K_{NO} is defined by eq 8;

$$\Delta A = \Delta\epsilon - [b - (b^2 - 4(K_{NO})^2[Fe]_0[NO]_0)^{1/2}/2K_{NO}] \quad (9)$$

$[Fe]_0$ and $[NO]_0$ are the analytical concentrations of the porphyrin and nitric oxide in solution, respectively. The results of the best fit of this quadratic equation to the data shown give $K_{NO} = (1.21 \pm 0.08) \times 10^3$ and $\Delta\epsilon = (1.56 \pm 0.02) \times 10^5$ M^{-1} cm^{-1}. Figure 5 shows the best-fit line according to eq 9.

Table 2. Half-Wave Potentials Determined by Cyclic Voltammetry

		$E_{1/2}$		
couple	solvent	measd	vs SHE	ref
$Fe^{II/III}$TpivPP(NO)(NO_2)	CH_3CN	+0.30[a]	+0.54	this work
$Fe^{II/III}$TpivPP(ClO_4)	CH_3CN	−0.95[a]	−0.71	this work
$Fe^{II/III}$TpivPP(NO)[c]	CH_3CN	+0.14[a]	+0.38	this work
$Fe^{II/III}$TpivPP(NO_2)	CH_3CN	−0.92[a]	−0.68	this work
$Fe^{II/III}$TpivPP(NO_2)$_2$	CH_3CN	−1.20[a]	−0.96	this work
$Fe^{II/III}$TpivPPCl	DMF	−0.103[b]	+0.138	33
$Fe^{II/III}$TPP(NO_2)$_2$	DMF	−0.45[b]	−0.21	30
$Fe^{II/III}$OEP(NO_2)$_2$	DMF	−0.83[b]	−0.59	30
$Fe^{II/III}$TPP(NO)[c]	py	+0.54[b]	+0.78	34
$Fe^{II/III}$OEP(NO)[c]	BuCN	+0.63[b]	+0.87	28
$Fe^{II/IIp+}$iBC(NO)	BuCN	+0.22[b]	+0.46	29
NO_2^-/NO_2	CH_3CN	+0.4[a,c]	+0.64	this work
NO_2^-/NO_2	CH_3CN	+0.45[e]	+0.69[g,h]	23
NO_2^-/NO_2	CH_3CN	+0.078[a,f]	+0.32[g]	24
NO_2^-/NO_2	CH_3CN		+0.4[i]	25
NO/NO^+	CH_3CN	+0.94[a]	+1.18	this work
NO/NO^+	CH_3CN	+1.28[b]	+1.52	26
NO/NO^+	CH_3CN	+0.82[a]	+1.06	23

[a] Measured potential vs $Ag/AgNO_{3(AN)}$. Corrections to SHE depend on the use of the internal reference ferrocene, as described in the text. [b] Measured potential vs SCE. [c] Irreversible oxidation; reported potential is $E_{p/a}$. [d] Irreversible reduction; reported potential is $E_{p/c}$. [e] Derived from voltammetric measurements of irreversible oxidation in acetonitrile. [f] Determined in acetonitrile by ac polarography, Pt electrode. [g] Converted to SHE by the same method used in this work. This assumes a consistent value of the $Ag/AgNO_{3(AN)}$ reference electrode. [h] Value used in thermochemical analysis. [i] Derived from measurements in aqueous media.

Electrochemistry. Electrochemical studies were designed to determine the reduction potential for the conversion of the ferric porphyrin species [Fe^{III}TpivPP(NO)(NO_2)] (**5**) to [Fe^{II}TpivPP(NO)(NO_2)]$^-$ (**2**), since this value was required for the thermochemical cycle used in evaluation of $\Delta G°_{(X/XO)}$ of eq 3, discussed below. Since this species is stable in solution under NO sparge as described, the reduction potential for the formation of [Fe^{II}TpivPP(NO)(NO_2)]$^-$ (**2**) could be measured without the difficulty of chemical preparation and isolation. To understand and support the assignment of the cyclic voltammetry of **5** as resulting in the formation of **2**, a general investigation of the electrochemistry of the simpler porphyrin derivatives and free ligands was necessary.

The cyclic voltammogram of free nitrite shows an irreversible oxidation wave at variable potentials in the vicinity of +0.4 V vs $Ag/AgNO_{3(AN)}$ = +0.64 V vs SHE. Also, a reversible oxidation occurs at +0.60 V vs $Ag/AgNO_{3(AN)}$ = +0.84 V vs SHE. The first values listed in Table 2 may be compared with those of Castellano et al.,[23] Salzberg,[24] and Eberson[25] that are

(20) Perchlorate coordination to FeTPP was investigated in the solution and solid states: Reed, C. A.; Mashiko, T.; Bentley, S. P.; Kastner, M. E.; Scheidt, W. R.; Spartalian, K.; Lang, G. *J. Am. Chem. Soc.* **1979**, *101*, 2948−2958. It was studied in solution in the following: Goff, H.; Shimmura, E. *J. Am. Chem. Soc.* **1980**, *102*, 31−37. Its unique UV−visible spectral features discussed in the first paper are consistent with the calculated molar absorptivites of Figure 6B. The evidence in the latter paper for equilibrium dissociation at perchlorate and porphyrin concentrations of about 1 mM each in THF and $CHCl_3$ solution are consistent with the value of the equilibrium constant determined here. A reviewer has pointed out the possibility of employing more weakly coordinating anions to avoid these complications. Considering the complications in spectral stability under the conditions of excess perchlorate, it appears that other competing association equilibria from contaminant water or solvent would continue to dominate the system in the absence of a more strongly coordinating ligand.

(21) Settin, M.; Fanning, J. C. *Inorg. Chem.* **1988**, *27*, 1431−1435.

(22) Yoshimura, T. *Inorg. Chim. Acta* **1984**, *83*, 17−21.

(23) Castellano, C. E.; Calandra, A. J.; Arvia, A. J. *Electrochim. Acta* **1974**, *19*, 701−712. This reference contains an unfortunate typographical error that switches the values for the potentials of the couples reported here: NO/NO^+ and NO_2^-/NO_2. The correct values are reported in Table 2, and their consistency with other reported values is apparent.

(24) Salzberg, H. W. *J. Electrochem. Soc.: Electrochem. Sci. Technol.* **1974**, *121*, 1451−1454.

(25) Eberson, L. *Acta Chem. Scand.* **1984**, *B38*, 439−459.

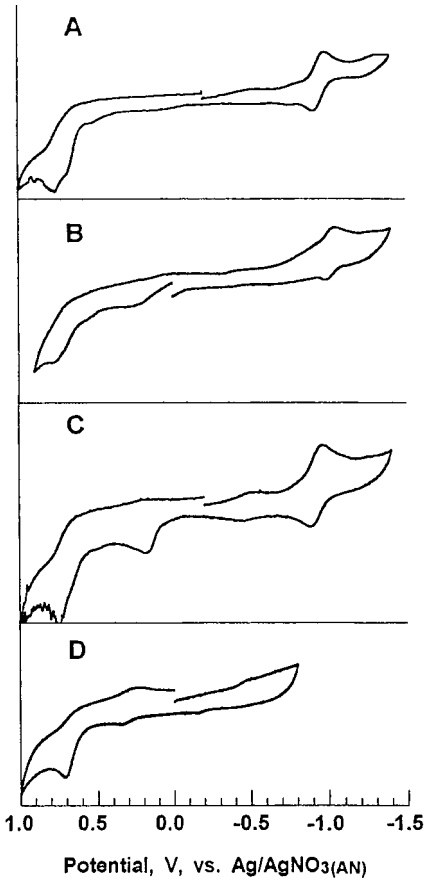

Figure 7. Cyclic voltammograms of (A) [Fe^{III}TpivPP(ClO_4)] under nitrogen, (B) [Fe^{II}TpivPP(NO)] with 0.15 mM NO, (C) [Fe^{III}TpivPP(ClO_4)(NO_2)] under nitrogen with analytical concentration of nitrite as (TPA)NO_2 = 0.12 mM, and (D) [Fe^{II}TpivPP(NO)(NO_2)] with 15 mM NO. All experiments are in acetonitrile with 0.050 M (TPA)ClO_4, a platinum working electrode, vs $Ag/AgNO_{3(AN)}$ reference electrode, at a scan rate = 20 mV/s. Porphyrin concentrations are 1×10^{-4} M in solution. Corrections to SHE are described in the text and Table 2.

also shown. Castellano's mechanistic study of nitrite oxidation reactions in acetonitrile appears to be the most thorough, and so we have used this value in our thermochemical calculations. That value of 0.69 V vs SHE, converted from the same reference electrode as used in this work, is quite close to the potential we observed for the irreversible oxidation.

Cyclic voltammetry of nitric oxide in the region of immediate interest revealed a reversible oxidation wave at +0.94 V vs $Ag/AgNO_{3(AN)}$ = +1.18 V vs SHE. This value, shown in Table 2, differs from that reported by Kochi and co-workers of +1.52 vs SHE in acetonitrile.[26] However, it agrees well with the potential of +1.06 vs SHE reported earlier by Castellano et al.

To obtain cyclic voltammograms of the iron porphyrins with nitro and nitrosyl ligands required preparation of the ferric species as outlined in eqs 6, 4b, and 8. The separate cyclic voltammograms of [Fe^{III}TpivPP(ClO_4)] (**7**), [Fe^{III}TpivPP(NO_2)(ClO_4)]$^-$ (**3b**), [Fe^{II}TpivPP(NO)] (**4**), and [Fe^{III}TpivPP(NO)(NO_2)] (**5**) are shown in Figure 7A−D. In Figure 7A, the cyclic voltammogram of **7** under nitrogen atmosphere with 0.050 M (TPA)ClO_4 shows a reversible reduction at −0.95 V vs the silver−silver nitrate electrode prepared in acetonitrile ($Ag/AgNO_{3(AN)}$). This value and the corresponding value of −0.71 V vs SHE are also shown in Table 2. The irreversible oxidation near +0.7 V vs $Ag/AgNO_{3(AN)}$ or 0.94 V vs SHE is attributed to ring oxidation[27] of the porphyrin. The value of K_0 and the concentration of electrolyte used ensure complete association of the perchlorate−porphyrin complex in this experiment.

The cyclic voltammogram of [Fe^{II}TpivPP(NO)] (**4**) in acetonitrile under an atmosphere of 1% NO with the same solvent, electrolyte, and reference electrode as in Figure 7A is shown in Figure 7B. The new feature, an irreversible oxidation with $E_{p/a}$ = +0.14 V vs $Ag/AgNO_{3(AN)}$ = +0.38 V vs SHE listed in Table 2, accompanies the original reversible wave of Figure 7A but with a smaller current. The value of the potential of the irreversible wave may be compared to the result of +0.78 V vs SHE obtained for [Fe^{II}TPP(NO)(py)] by Kadish[28] also listed in Table 2. Similar results of 0.87 V vs SHE for [Fe^{II}OEP(NO)] in butyronitrile (BuCN) are also given in Table 2. In the latter study, Fujita and Fajer[29] identified the oxidation as metal-centered, in contrast to ring-centered oxidations observed at this stage for analogous isobacteriochlorins (iBC) or sirohemes, which are generally ring-oxidized at less positive potentials than the porphyrins.

The current of the oxidation wave at +0.14 V vs $Ag/AgNO_{3(AN)}$ in Figure 7B is comparable to the reversible reduction at $E_{p/c}$ = −1.06 V vs $Ag/AgNO_{3(AN)}$ = −0.82 V vs SHE. For comparison, the nitrosyliron(II) TPP and OEP analogues showed reversible reductions to the [Fe^{I}P(NO)] species at −0.98 V vs SCE = -0.74 vs SHE and at −1.10 V vs SCE = −0.86 V vs SHE, respectively.

Since the irreversible oxidation of [Fe^{II}TpivPP(NO)] occurs at a potential that is 400 mV cathodic of the previously assigned metal-centered irreversible oxidation waves, a metal-centered oxidation is suggested for this case, too, rather than a ring oxidation. The similarity of the potentials for reduction among these porphyrins supports the irreversible formation of the [Fe^{I}TpivPP(NO)] derivative at −0.82 V vs SHE.

The cyclic voltammetry of [Fe^{III}TpivPP(NO_2)(ClO_4)] (**3a**) in the same medium is shown in Figure 7C. The irreversible wave observed at +0.18 V vs $Ag/AgNO_{3(AN)}$ differs from the potential of 0.4 V for irreversible oxidation of free nitrite measured separately in solution under the same conditions. The second irreversible wave at +0.75 V is also inconsistent with the cyclic voltammetry of free nitrite, which has a second reversible wave at +0.60 V, already discussed. Upon addition of more than 1 equiv of nitrite, however, these irreversible waves continue to grow in current intensity. The irreversible wave at +0.75 V vs $Ag/AgNO_{3(AN)}$ = +1.38 V vs SHE gradually shifts to show the expected reversibility and potential of free nitrite as excess nitrite is added, but the irreversible wave remains unshifted from the potential observed for the nitro complex and, as expected, remains irreversible. With the clear dependence of current magnitude on the concentration of nitrite for these waves, it is apparent that they correspond both to free and coordinated nitrite oxidation.

The reversible reduction observed for [Fe^{III}TpivPP(NO_2)(ClO_4)] (**3a**), centered at −0.92 V vs $Ag/AgNO_{3(AN)}$ = −0.68 V vs SHE, is assigned as the metal-centered reduction, Fe(III)/Fe(II), due to the closeness of this value to that for the reversible reduction of the simple perchlorate derivative, **7**. For the dinitroiron(III) porphyrin derivative **1a**, generated upon addition of excess nitrite, this reversible wave is cathodically shifted to −1.20 V vs $Ag/AgNO_{3(AN)}$ = −0.96 V vs SHE. These results may be compared with those for the FeTPP derivative obtained

(26) Lee, K. Y.; Kuchynka, D. J.; Kochi, J. K. *Inorg. Chem.* **1990**, *29*, 4196−4204.

(27) Barley, M. H.; Takeuchi, K. J.; Meyer, T. J. *J. Am. Chem. Soc.* **1986**, *108*, 5876−5885.

(28) Kadish, K. M. In *Iron Porphyrins*; Lever, A. B. P., Gray, H. B., Eds.; Addison-Wesley: Reading, MA, 1983; Part II.

(29) Fujita, E.; Fajer, J. *J. Am. Chem. Soc.* **1983**, *105*, 6743−6745.

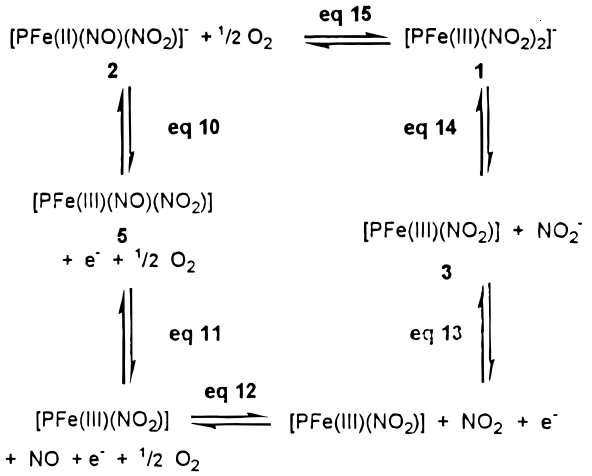

Figure 8. Thermochemical cycle for determination of $\Delta G^\circ_{(X/XO)}$ for the conversion of $[Fe^{II}TpivPP(NO)(NO_2)]^-$ (**2**) to $[Fe^{III}TpivPP(NO_2)_2]^-$ (**1**), as shown in eq 15.

Table 3. Free Energy Changes (kJ/mol) for Oxo Transfer Reactions

couple (X/XO)	$\Delta G^\circ_{(X/XO)}$	medium	ref	ΔG°_{trans}[a]
$[FeP(NO)(NO_2)]^-/[FeP(NO_2)_2]^-$ [b]	−50	CH_3CN	this work	
Ph_3P/Ph_3PO[c]	−268	1,2-dichloroethane	35	−213[d]
NO_2^-/NO_3^-	−121	1,2-dichloroethane	25	−71
O_2/O_3	+163.2	gas	31	+213

[a] For the reaction of the $[Fe^{III}TpivPP(NO_2)_2]^-$ anion XO with X′. [b] As written in eq 15. [c] As written in eq 2. [d] As written in eq 1.

by Ryan and co-workers.[30] In that study, mononitroiron porphyrins were not observed in isolation due to the magnitude of the stability constants and the concentrations used in the experiments. The half-wave potentials for the dinitro species, $[FeTPP(NO_2)_2]^-$ and $[FeOEP(NO_2)_2]^-$, are given in Table 2 as −0.21 and −0.59 V, respectively, and contrast with the value of −0.96 V (all vs SHE) observed in this work.

Figure 7D shows the cyclic voltammogram of a solution of **3a**, of Figure 7C, sparged with 1% NO, which gives a concentration of 0.15 mM NO. The reversible formation of **6** under these conditions gives rise to a cyclic voltammogram which shows a unique reversible wave at +0.30 V vs $Ag/AgNO_{3(AN)}$ = +0.54 V vs SHE. The comparable magnitudes of the oxidizing and reducing currents for this wave suggest that they arise from the same porphyrin species. The irreversible wave at +0.75 V is similar to the waves observed in Figure 7A,B and is attributed to oxidation of the uncomplexed and monosubstituted porphyrins in solution in addition to the mixed ligand species.

Certain assignment of the reversible wave as metal-centered oxidation/reduction, that is, Fe(II)/Fe(III), or as ligand-centered, $Fe^{III}(NO)(NO_2)/Fe^{III}(NO)(NO_2)^+$, is not possible within the limited scope of these experiments. However, it is likely that the metal-centered oxidation potential is dominated by the nitrosyl ligand as it is in $[Fe^{II}TPP(NO)]$, $[Fe^{II}OEP(NO)]$, and $[Fe^{II}TpivPP(NO)]$. This new reversible oxidation wave is similar to the potentials for the irreversible metal-centered oxidations for these simple nitrosyl complexes and is also assigned as such.

Thermochemistry. With the electrochemical and equilibrium data, a thermochemical cycle was constructed to estimate the change in free energy associated with oxo transfer. The thermochemical cycle sketched in Figure 8 indicates both literature values and measured values used for this analysis by reference to eqs 10−14, in which P is used to designate the picket fence porphyrin. Values for gas phase reactions and for

$$[Fe^{II}P(NO)(NO_2)]^- \rightarrow [Fe^{III}P(NO)(NO_2)] + e^- \quad (10)$$

$E_{1/2}$ = 0.54 V vs SHE (CH_3CN, this work)

$$[Fe^{III}P(NO)(NO_2)] \rightarrow [Fe^{III}P(NO_2)] + NO_{(AN)} \quad (11)$$

$1/K_{NO} = (8.26 \pm 0.5) \times 10^{-4}$ M^{-1}

$\Delta\epsilon = (1.56 \pm 0.02) \times 10^5$ M^{-1} cm^{-1}

ΔG° = 18 kJ/mol (CH_3CN, this work)

$$NO_{(g)} + {}^1/_2O_{2(g)} \rightarrow NO_{2(g)} \quad (12)$$

ΔG° = −35.2 kJ/mol (gas phase)[31]

$$e^- + NO_{2(AN)} \rightarrow {NO_2}^-_{(AN)} \quad (13)$$

$E_{1/2}$ = 0.69 V vs SHE (CH_3CN)[23]

$$NO_2^- + [Fe^{III}P(NO_2)] \rightarrow [Fe^{III}P(NO_2)_2]^- \quad (14)$$

$K_2 = 2.18 \times 10^3$ ΔG° = −19.0 kJ/mol (CH_3CN, this work)

reactions in other solvent systems were used in the absence of those for acetonitrile solution. No corrections for these phase differences were made. Combining eqs 10 and 13 provides the free energy for the electron transfer reaction embedded in this cycle as ΔE = 0.15 V, ΔG° = −14 kJ/mol. Combining eqs 10−14 gives the oxo-transfer reaction of eq 15, and summation of the free energies provides its free energy as −50 kJ/mol.

$$[Fe^{II}TpivPP(NO)(NO_2)]^- + {}^1/_2O_2 \rightarrow [Fe^{III}TpivPP(NO_2)_2]^- \quad (15)$$

Equation 15 is the reverse of eq 3, and it is written in this form to be consistent with the implied reaction for $\Delta G^\circ_{(X/XO)}$ values as reported in Table 3.

In combining these results for eq 15 with oxo-transfer half-reaction data from the literature, a variety of oxo-transfer reaction energies may be calculated. Table 3 lists literature values of $\Delta G^\circ_{(X/XO)}$ and calculated oxo-*transfer* reaction energies for the model reaction with triphenylphosphine of eq 1 as −218 kJ/mol. For the oxo-transfer reactions of $[Fe^{III}TpivPP(NO_2)_2]^-$ with free nitrite and dioxygen, the oxo-transfer free energies are calculated as −71 and +213 kJ/mol, respectively. Therefore, the contrasting reactivity of the dinitroiron(III) picket fence porphyrin anion with dioxygen is consistent with its thermochemistry and raises compelling questions about the thermochemistry of the chloronitroiron(III) tetraphenylporphyrin anion in its oxidation of dioxygen. The moderately favorable driving force for reduction of free nitrite by the dinitroiron(III) picket fence porphyrin is notable, given the porphyrin's apparent stability in solutions of excess nitrite. It should be pointed out, that in analogous anaerobic solutions of nitro derivatives of

(30) Fernandes, J. B.; Feng, D.; Chang, A.; Keyser, A.; Ryan, M. D. *Inorg. Chem.* **1986**, *25*, 2606−2610.

(31) *The NBS Tables of Chemical Thermodynamic Properties*; Lide, D. R., Ed.; Journal of Physical and Chemical Reference Data 11, Supplement 2; American Chemical Society and the American Institute for Physics: Washington, DC, 1974; p 311.

Fe(III)TPP that had no other axial ligand such as the chloro ligand, there has been a report of direct oxo transfer between the coordinated nitro ligand and free nitrite to produce nitrate.[32] Continuing thermochemical analyses of the remarkable differences in reactivity between the simple porphyrins and the picket fence porphyrin derivatives are underway, with particular attention given to the effects of the presence and identity of trans axial ligands.

Acknowledgment. Preliminary work was carried out at Auburn University under an NSF-ROA supplementary grant to David M. Stanbury and J.A.G. Local award of Howard Hughes Medical Institute summer research funds at Eckerd College supported J.G., M.D., M.B., A.J., and J.P. and the purchase of minor equipment. Acknowledgment is made to the donors of The Petroleum Research Fund, administered by the ACS, and to Research Corp. for funding in support of this work. We also graciously thank W. R. Scheidt, Habib Nasri, and Mark Mashuta of the University of Notre Dame for their support in the preliminary work. Thanks are also due to D. R. McMillin of Purdue University for supplying us with a copy of the SPECDEC program and to Jim Myers of Eckerd College for essential technical support in fabrication of equipment.

IC9608915

(32) Finnegan, M. G.; Lappin, A. G.; Scheidt, W. R. *Inorg. Chem.* **1990**, *29*, 181.
(33) Lexa, D.; Momenteau, M.; Rentieu, P.; Rytz, G.; Savéant, J.-M.; Xu, F. *J. Am. Chem. Soc.* **1984**, *106*, 4755−4765.
(34) Olson, L. W.; Schaeper, D.; Lancon, D.; Kadish, K. M. *J. Am. Chem. Soc.* **1982**, *104*, 2042−2044.
(35) This value was derived from evaluation of $\Delta H°$ values of half-reactions: Holm, R. *Chem. Rev.* **1987**, *87*, 1401−1499. An estimated correction of 5 kcal/mol = $T\Delta S°$ at 25 °C was made in arriving at this $\Delta G°$ approximation.